J. Parasitol., 98(3), 2012, pp. 572–583

SYNOPTIC REVISION OF *BLABERICOLA* (APICOMPLEXA: EUGREGARINIDA: BLABERICOLIDAE) PARASITIZING BLABERID COCKROACHES (DICTYOPTERA: BLABERIDAE), WITH COMMENTS ON DELINEATING GREGARINE SPECIES BOUNDARIES

Richard E. Clopton
Department of Natural Science, Peru State College, Peru, Nebraska 68421. *e-mail: rclopton@oakmail.peru.edu*

ABSTRACT: Complete synoptic redescriptions, including complete morphometric data for all life cycle stages, species recognition characters, and differential comparisons are presented for the 4 gregarine species comprising *Blabericola*. *Blabericola cubensis* (Peregrine, 1970), *Blabericola haasi* (Geus, 1969), *Blabericola migrator* (Clopton, 1995), and *Blabericola princisi* (Peregrine, 1970) are redescribed from their type hosts, i.e., the discoid cockroach *Blaberus discoidalis*, the lobster cockroach *Nauphoeta cinerea*, the Madagascar hissing cockroach *Gromphadorhina portentosa*, and the Bolivian cockroach *Blaberus boliviensis*, respectively. These gregarine species descriptions are stabilized through deposition of extensive new voucher collections. Species of *Blabericola* are distinguished by differences in relative metric ratios, morphology of oocysts, and by relative metric ratios of mature gamonts in association. This work is discussed as a model for morphological species descriptions in the Eugregarinorida including the 6 principles for morphological gregarine species descriptions, i.e., a centroid and population variation approach, adequate sample size, partitioning developmental variation and sexual dimorphism, recognition and minimization of fixation and physiological artifacts to eliminate false morphotypes, and comparative data sets across multiple life cycle stages.

The Blabericolidae comprises 2 gregarine genera, *Protomagalhaensia* Pinto, 1918 and *Blabericola* Clopton, 2009. These genera include 9 known gregarine species hypothesized to represent a vicariant assemblage rising through parallel sequential speciation and radiation subsequent to radiation and speciation by their host cockroach lineage (Clopton, 2009). Molecular sequence data support a co-evolutionary model as well as the monophyly of *Protomagalhaensia*, *Blabericola*, and Blabericolidae (Clopton, 2009; Rueckert et al., 2011). Although the cockroaches (Dictyoptera: Blattaria) are a cosmopolitan insect group comprising over 4,000 named species (Roth, 1983) and commonly infected by gregarine parasites, less than a dozen putative blabericolid species have been described from cockroaches worldwide and most are poorly known. Clopton (2011) described or redescribed and delineated 3 of the 5 gregarine species comprising *Protomagalhaensia*, but the 4 known species of *Blabericola* need synoptic redescription and deposition of new (voucher) specimen series to stabilize the genus and its member taxa.

Clopton (2009) erected *Blabericola* to unite 4 known gregarine species based on molecular, morphological, and life cycle characters. *Blabericola migrator* (Clopton, 1995), described from *Gromphadorhina portentosa* Brunner von Wattenwyl, 1865 (Dictyoptera: Blattaria: Blaberidae: Oxyhaloinae: Gromphadorhini), was originally placed within *Leidyana* Watson, 1915. *Blabericola haasi* (Geus, 1969), described from *Nauphoeta cinerea* (Olivier, 1789) (Dictyoptera: Blattaria: Blaberidae: Oxyhalinae: Nauphoetini), was originally placed within *Gregarina* Dufour, 1828 and was later moved to *Leidyana* by Clopton and Hays (2006). *Blabericola cubensis* (Peregrine, 1970), described from *Blaberus discoidalis* Serville, 1839 (Dictyoptera: Blattaria: Blaberidae: Blaberinae), and *Blabericola princisi* (Peregrine, 1970), described from *Blaberus boliviensis* Princis, 1946 (Dictyoptera: Blattaria: Blaberidae: Blaberinae), were originally placed within *Gregarina*. Type material for *B. haasi* is sufficient to stabilize the species and allow redescription (1 neotypical hapantotype slide and 84 accompanying slides from the series, Clopton and Hays, 2006), but type material for the remaining species of *Blabericola* is limited. Type material for *B. migrator* is limited to 8 slides (Clopton, 1995). Type material for *B. cubensis* and *B. princisi* is limited to 1 slide each (Peregrine, 1970), but both slides exhibit extreme fixation artifacts that render the specimens essentially useless for taxonomy.

Taxonomic progress in *Blabericola* requires redescription and stabilization of its known member species. Herein, I provide synoptic redescription and differentiation of *B. cubensis*, *B. haasi*, *B. migrator*, and *B. princisi* and document the deposition of new voucher material to stabilize these taxa. Using this work as a model, I also address the role of morphology in gregarine species delineation.

MATERIALS AND METHODS

Gregarines cultures were maintained in breeding colonies of *B. boliviensis*, *B. discoidalis*, *G. portentosa*, and *N. cinerea* housed in 22-L polycarbonate containers with coir bedding and cardboard egg-crate roosting habitat. Dry dog food and water were provided ad libitum. Adult and late-instar nymphal cockroaches were examined for gregarine parasites as described by Clopton (2010, 2011). Permanent microscope slide preparations of gregarines were made using techniques detailed by Clopton and Hays (2006) and references therein. Gametocyst development utilized the methods described by Clopton (2011) while oocyst studies followed the techniques of Clopton (2010). Gregarine DNA samples were prepared and stored for future genomic analysis using a procedure described by Clopton (2011). New, and complete, synoptic morphometric data sets, including gametocysts, oocysts, and mature gamonts were collected for all known species of *Blabericola* using the equipment and software reported by Clopton (2011).

This work utilizes a revised set of extended morphometric character sets for mature gamonts and oocysts of *Blabericola* (Figs. 1–3) (see Clopton and Hays, 2006; Clopton, 2010, 2011). The following metric characters and abbreviations were used: length of deutomerite (DL); distance from protomerite-deutomerite septum to deutomerite axis of maximum width (DLAM); distance from posterior end of deutomerite to deutomerite axis of maximum width (DLPM); width of deutomerite at equatorial axis (DWE); maximum width of deutomerite (DWM); length of gametocyst (GL); width of gametocyst (GW); diameter of major karyosome (KD); distance from nucleus to protomerite-deutomerite septum (NDS); length of nucleus (NL); width of nucleus (NW); interior oocyst length (OLI); maximum exterior oocyst length (OLM); maximum oocyst width (OW); width of protomerite-deutomerite septum (PDSW); length of protomerite (PL); distance from anterior end of protomerite to protomerite axis of maximum width (PLAM); distance from protomerite-deutomerite septum to protomerite axis of maximum width (PLPM); width of primite-satellite septal junction (PSSW); length of oocyst polar plate (PPL); width of oocyst polar plate (PPW); total length of primite (PTL); width of protomerite at equatorial axis (PWE); maximum width of protomerite (PWM); oocyst residuum diameter (ResDia); total length of satellite

Received 4 October 2011; revised 30 November 2011; accepted 12 December 2011.
DOI: 10.1645/GE-3000.1

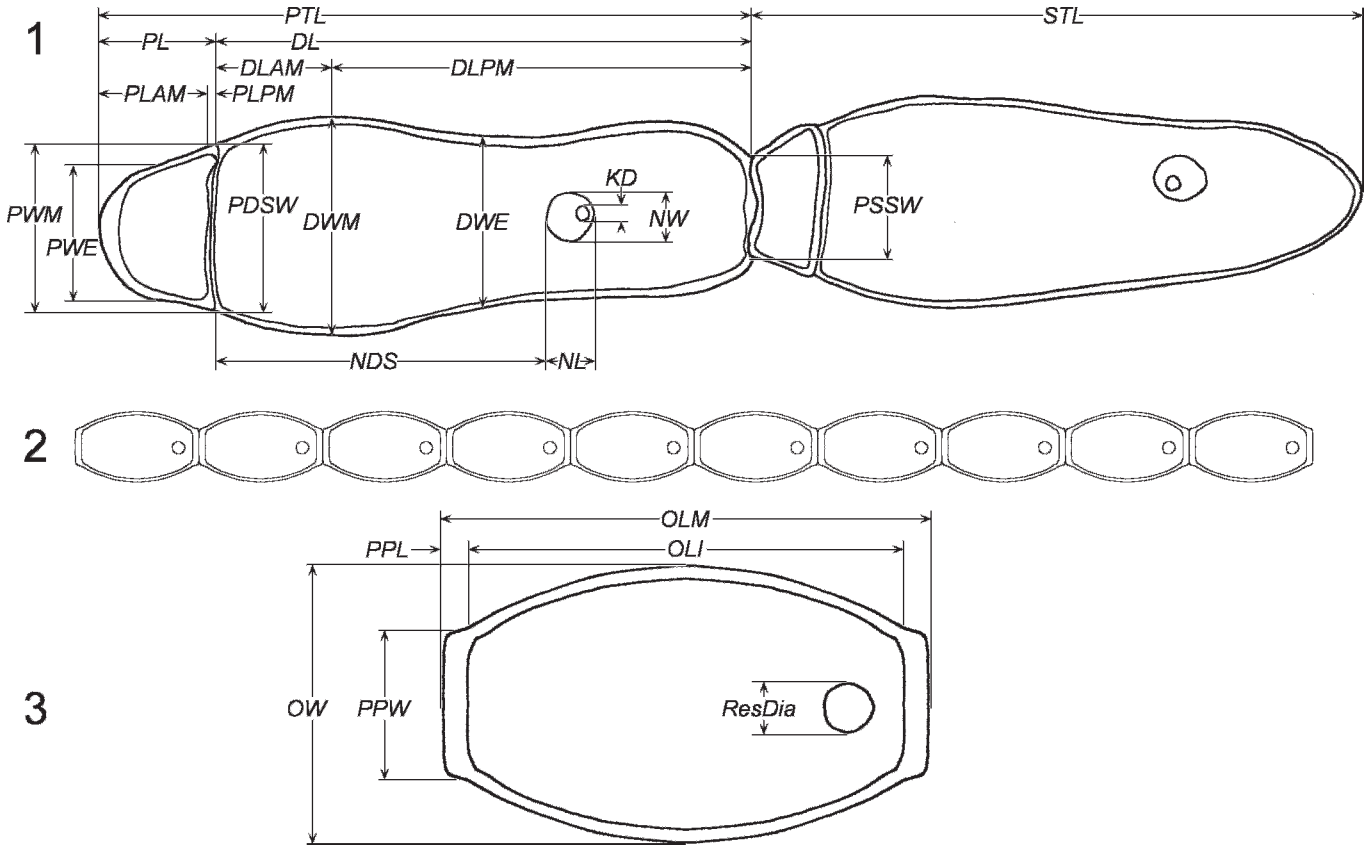

FIGURES 1–3. Morphometric character set for gamonts and oocysts of *Blabericola* species. (**1**) Primite (left) and satellite (right) gamonts forming a mature association. Generalized characters are mapped onto the primite. (**2**) Monete oocyst chain. (**3**) Oocyst. Length of deutomerite (DL); distance from protomerite-deutomerite septum to deutomerite axis of maximum width (DLAM); distance from posterior end of deutomerite to deutomerite axis of maximum width (DLPM); width of deutomerite at equatorial axis (DWE); maximum width of deutomerite (DWM); length of gametocyst (GL); width of gametocyst (GW); diameter of major karyosome (KD); distance from nucleus to protomerite-deutomerite septum (NDS); length of nucleus (NL); width of nucleus (NW); interior oocyst length (OLI); maximum exterior oocyst length (OLM); maximum oocyst width (OW); width of protomerite-deutomerite septum (PDSW); length of protomerite (PL); distance from anterior end of protomerite to protomerite axis of maximum width (PLAM); distance from protomerite-deutomerite septum to protomerite axis of maximum width (PLPM); width of primate-satellite septal junction (PSSW); length of oocyst polar plate (PPL); width of oocyst polar plate (PPW); total length of primite (PTL); width of protomerite at equatorial axis (PWE); maximum width of protomerite (PWM); oocyst residuum diameter (ResDia); total length of satellite (STL); total length (TL). Primite (P) and satellite (S) abbreviations are prefixed to existing abbreviations to differentiate the same metric across sexes (e.g., total length of primite [PTL], total length of satellite [STL]).

(STL); and total length (TL). Primite (P) and satellite (S) abbreviations are prefixed to existing abbreviations to differentiate the same metric across sexes, e.g., total length of primite (PTL) and total length of satellite (STL).

The shapes of structures in mature trophozoites, particularly the epimerite, comprise an important diagnostic character suite, but significant developmental variation within taxa precludes the use of absolute metrics taken from trophozoites (Filipponi, 1951; Watwood et al., 1997; Clopton, 1999). Separate description of primite and satellite ontogenic stages are provided to account for the sexual dimorphism (Filipponi, 1947, 1951, 1952, 1954, 1955). Measurements are presented in micrometers as mean values followed parenthetically by range values, standard deviations, and sample sizes. Metric differences between species were identified using ANOVA-protected Tukey's honestly significant difference tests ($\alpha = 0.05$). Parasite ontogenetic and anatomical nomenclature largely follows that proposed by Levine (1971), but defer to Clopton (2009) in reference to association, syzygy, gametocyst development, and oocyst dehiscence. Nomenclature for the shapes of planes and solids follows Clopton (2004).

REDESCRIPTIONS

Blabericola Clopton, 2009

Diagnosis: Order Eugregarinorida Léger, 1892, sensu Clopton (2002); Suborder Septatorina Lankester, 1885, sensu Clopton (2002); Superfamily Gregarinoidea, Chakaravarty, 1960 emend Clopton (2009); Family Blabericolidae Clopton, 2009; with the characters of the genus *Blabericola* Clopton, 2009 as follows: epimerite simple, globular to pyriform, without diamerite; deutomerite of gamont obpanduriform; association gamontic, presyzygial, caudofrontal; gametocysts with spore tubes, dehiscing by extrusion of monete oocyst chains; oocysts elliptoid to dolioform; parasites of blaberid cockroaches.

Taxonomic summary

Type species: Blabericola migrator (Clopton, 2005) Clopton, 2009.

Blabericola cubensis (Peregrine, 1970) Clopton, 2009

(= *Gregarina cubensis* Peregrine, 1970)
(Figs. 4–11)

Trophozoite (Fig. 7): Young trophozoites solitary, extracellular forms attached to host ventricular epithelium. Holdfast a narrowly obpanduriform epimerite without diamerite. Protomerite very broadly ovoid, markedly constricted at protomerite-deutomerite septum. Deutomerite narrowly obpanduriform. Nucleus orbicular with nearly orbicular, smooth-margined, eccentric karyosome.

Association (Figs. 8–11): Presyzygial, gamontic; gamonts anisomorphic due to structures involved in association interface; association interface a shallow interlock, posterior end of primite's deutomerite embedded in shallow torus formed from anterior membranes of satellite's protomerite.

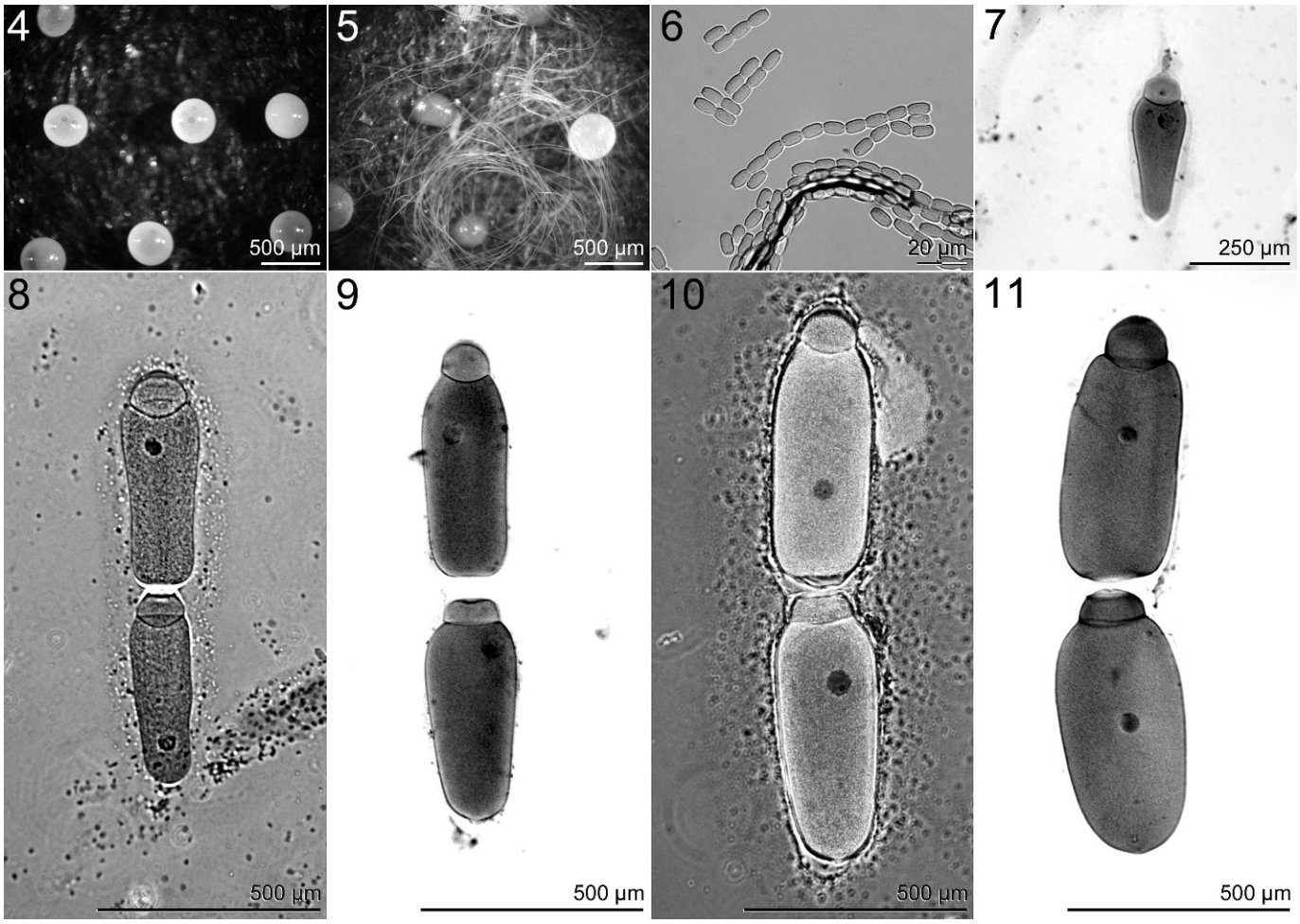

FIGURES 4–11. *Blabericola cubensis*. (**4**) Gametocysts. (**5**) Monete oocyst chains dehisced from mature gametocysts. (**6**) Oocysts. (**7**) Solitary trophozoite with epimerite. (**8**–**11**) Variation in typical mature associations.

Measurements taken from mature gamonts in association. Indices: PTL/STL 1.12 (0.98–1.30, ±0.09, 30), PPL/SPL 1.65 (1.13–2.43, ±0.31, 30), PPWM/SPWM 1.02 (0.89–1.24, ±0.09, 30), PDL/SDL 1.04 (0.93–1.20, ±0.08, 30), PDWM/SDWM 1.06 (0.93–1.20, ±0.07, 30), PDWE/SDWE 1.07 (0.90–1.29, ±0.10, 30).

Primite: Observations and data taken from mature primites in association. Epimerite absent; protomerite very broadly ovoid to very broadly subelliptoid; PL 102.6 (84.5–125.5, ±9.67, 30), PWE 105.6 (95.3–124.6, ±6.24, 30), PWM 119.5 (109.1–143.5, ±7.51, 30), PLAM 65.0 (18.1–89.6, ±19.19, 30), PLPM 36.8 (13.8–80.9, ±16.36, 30), PDSW 118.3 (104.5–137.2, ±7.03, 30), PL/PWE 0.98 (0.81–1.23, ±0.11, 30), PL/PWM 0.86 (0.73–1.07, ±0.09, 30), PL/PDSW 0.87 (0.69–1.10, ±0.09, 30), PLAM/PL 0.63 (0.17–0.84, ±0.17, 30), PLAM/PLPM 2.21 (0.22–5.30, ±1.12, 30), PWM/PWE 1.13 (1.01–1.23, ±0.05, 30). Deutomerite narrowly obpanduriform, (approaching oblong to narrowly oblong in largest specimens as artifact of coverslip compression); DL 459.4 (404.4–521.1, ±29.52, 30), DWE 167.7 (142.1–203.2, ±13.51, 30), DWM 180.4 (162.7–202.2, ±10.65, 30), DLAM 164.8 (52.1–392.8, ±117.52, 30), DLPM 293.7 (77.1–432.7, ±126.26, 30), DL/DWE 2.76 (2.18–3.18, ±0.27, 30), DL/DWM 2.55 (2.11–2.90, ±0.19, 30), DLAM/DL 0.36 (0.11–0.84, ±0.26, 30), DLAM/DLPM 1.25 (0.12–5.09, ±1.75, 30), DWM/DWE 1.08 (0.99–1.20, ±0.05, 30), PTL 561.0 (492.0–630.4, ±34.08, 30). Indices: PTL/PL 5.49 (4.71–6.18, ±0.41, 30), PTL/PWM 4.71 (4.11–5.40, ±0.34, 30), PTL/PWE 5.33 (4.58–5.98, ±0.37, 30), DL/PL 4.50 (3.75–5.15, ±0.39, 30), PTL/DL 1.22 (1.20–1.26, ±0.02, 30), PTL/DWM 3.12 (2.65–3.48, ±0.22, 30), PTL/DWE 3.37 (2.64–3.86, ±0.32, 30), DWM/PWM 1.51 (1.33–1.74, ±0.10, 30), DWE/PWE 1.08 (0.99–1.20, ±0.05, 30). Nucleus nearly orbicular with a single, eccentric orbicular karyosome and varying smaller endosomes; NL 56.5 (41.8–72.2, ±6.51, 30), NW 53.2 (33.4–68.7, ±7.98, 30), NDS 170.7 (7.4–393.7, ±146.57, 30), KD 19.8 (11.8–32.3, ±4.17, 30), NL/NW 1.07 (1.00–1.48, ±0.09, 30), NDS/NL 3.03 (0.15–6.71, ±2.61, 30), DL/NDS 11.02 (1.20–63.24, ±15.88, 30), NL/KD 2.93 (1.97–4.16, ±0.49, 30).

Satellite: Observations and data taken from mature satellites in association. Protomerite compressed anteriorly by association interface, very shallowly dolioform to depressed oblong, anterior membranes forming toroidal margin at association interface; PSSW 98.1 (75.2–119.7, ±10.63, 30), PL 63.9 (46.3–87.3, ±10.73, 30), PWE 107.7 (89.2–122.7, ±8.38, 30), PWM 117.2 (104.8–130.0, ±7.36, 30), PLAM 39.4 (15.4–56.1, ±10.92, 30), PLPM 23.9 (9.0–47.0, ±10.32, 30), PDSW 115.0 (103.5–128.0, ±7.22, 30), PL/PWE 0.59 (0.42–0.91, ±0.10, 30), PL/PWM 0.55 (0.38–0.77, ±0.09, 30), PL/PDSW 0.56 (0.40–0.78, ±0.09, 30), PLAM/PL 0.62 (0.24–0.86, ±0.15, 30), PLAM/PLPM 2.02 (0.33–5.32, ±1.05, 30), PWM/PWE 1.09 (1.00–1.18, ±0.05, 30). Deutomerite very deeply to narrowly obovoid, (approaching nearly elliptoid in largest specimens as artifact of coverslip compression); DL 442.0 (409.0–478.4, ±20.29, 30), DWE 157.8 (120.8–174.9, ±12.66, 30), DWM 170.9 (147.1–188.9, ±10.02, 30), DLAM 149.2 (67.4–384.9, ±115.06, 30), DLPM 292.1 (68.5–402.5, ±116.97, 30), DL/DWE 2.82 (2.44–3.92, ±0.29, 30), DL/DWM 2.59 (2.28–3.22, ±0.20, 30), DLAM/DL 0.34 (0.15–0.85, ±0.26, 30), DLAM/DLPM 1.20 (0.18–5.62, ±1.86, 30), DWM/DWE 1.09 (1.01–1.22, ±0.05, 30), STL 503.8 (465.2–535.0, ±19.57, 30). Indices: STL/PL 8.08 (5.84–11.36, ±1.28, 30), STL/PWM 4.31 (3.83–4.80, ±0.20, 30), STL/PWE 4.70 (4.14–5.33, ±0.31, 30), DL/PL 7.12 (4.84–10.34, ±1.28, 30), STL/DL 1.14 (1.10–1.21, ±0.03, 30), STL/DWM 2.96 (2.69–3.53, ±0.19, 30), STL/DWE 3.21 (2.77–4.30, ±0.29, 30), DWM/PWM 1.46 (1.30–1.65, ±0.09, 30), DWE/PWE 1.47 (1.19–1.77, ±0.13, 30). Nucleus nearly orbicular with single, eccentric orbicular karyosome; NL 52.5 (40.6–65.1,

±5.98, 30), NW 48.5 (36.1–58.8, ±5.75, 30), NDS 228.6 (23.5–355.5, ±109.11, 30), KD 18.9 (11.8–30.4, ±3.42, 30), NL/NW 1.09 (1.00–1.25, ±0.07, 30), NDS/NL 4.35 (0.38–6.88, ±2.00, 30), DL/NDS 3.19 (1.25–19.21, ±3.65, 30), NL/KD 2.84 (1.85–3.73, ±0.45, 30).

Gametocysts (Figs. 4–5): White, opaque, irregularly orbicular, length 457.1 (412.0–510.0, ±31.53, 30), width 437.0 (388.0–497.0, ±29.69, 30), GL/GW 1.00 (1.00–1.10, ±0.04, 30). Gametocysts collected and stored under moist conditions dehisced within 24–36 hr, releasing oocysts in monete chains by extrusion.

Oocysts (Figs. 5–6): Dolioform with outline smoothing to incorporate terminal polar plates, single oocyst residuum simple, smooth, orbicular, nearly terminal; OLM 9.3 (9.1–9.5, ±0.13, 30), OLI 8.1 (8.0–8.3, ±0.12, 30), OW 5.2 (5.1–5.3, ±0.07, 30), PPW 3.1 (2.7–3.4, ±0.19, 30), PPL 0.6 (0.4–0.8, ±0.10, 30), ResDia 0.9 (0.7–1.2, ±0.13, 30), OLM/OLI 1.80 (1.70–1.90, ±0.04, 30), OLM/OW 1.80 (1.70–1.90, ±0.04, 30), OLI/OW 1.60 (1.50–1.60, ±0.03, 30), PPW/PPL 5.50 (3.80–9.20, ±1.23, 30), OW/PPW 1.70 (1.50–1.90, ±0.11, 30), OLM/PPL 16.10 (12.10–25.40, ±3.09, 30), OLM/ResDia 10.80 (7.60–13.60, ±1.50, 30), OW/ResDia 6.10 (4.20–7.90, ±0.88, 30).

Taxonomic summary

Type host: Blaberus discoidalis Serville, 1839 (Dictyoptera: Blattaria: Blaberidae: Blaberinae), nymphs and adults.

Type locality: Laboratory cultures, Department of Zoology, University College Cardiff (Cardiff University), Cardiff, Wales, United Kingdom.

Type specimens: Holotype is an hapantotype slide, registration number 1970:3:3:1, The Natural History Museum, London, England, U.K.

Site of infection: Trophozoites were collected from ventricular cecae and post-intercecal region. Associations were collected from the anterior mesenteron. Gametocysts were collected from host feces.

Prevalence: Prevalence in colony approaches 100%.

Records: Laboratory cultures, nymphs, and adults, Peru State College, Peru, Nebraska.

Specimens deposited: The voucher slide series for this redescription is deposited in the Harold W. Manter Laboratory for Parasitology (HWML), Division of Parasitology, University of Nebraska State Museum, Lincoln, Nebraska and comprises 56 hapantotype slides containing multiple trophozoites, gamonts, and associations accessioned as HWML100045.

Remarks

Blabericola cubensis is readily distinguished from *B. haasi* and *B. migrator* by significant differences in overall size and shape of gamonts in association (cf. Figs. 8–11 with Figs. 16–19 and Figs. 24–27, respectively; Figs. 36–39), by all metric measures observed except PriNDS, SatPL, and SatNW, which were not significantly different from those of *B. migrator*. In general, gamonts of *B. cubensis* are larger than those of *B. haasi* but smaller than those of *B. migrator* by all significant metrics. Gamonts of *B. cubensis* are most similar to those of *B. princisi* (cf. Figs. 8–11 with Figs. 32–35; Figs. 36–39) but exhibit consistently and significantly larger PriPWE, PriDWE, PriDWM, PriNL, PriNW, PriKD, PSSW, SatPWE, SatPWM, SatPDSW, SatNL, and SatKD metrics. In general, gamonts of *B. cubensis* possess deutomerites that are broader and less obviously obpanduriform than those of *B. princisi.* The primite protomerites are elliptoid or ovoid in *B. cubensis* but deltoid in *B. princisi*. Centroid clustering diagrams of differential gamont metrics (Figs. 36–39) readily demonstrate significant differences between all 4 species while illustrating the significant metric overlap of *B. cubensis* and *B. princisi*. The toroidal margin of the primite-satellite interface formed by the anterior membranes of the satellite protomerite is much less pronounced in *B. cubensis* than in *B. princisi* (cf. Figs. 8–11 and 32–35, respectively). This difference was also noted by Peregrine (1970) in her original descriptions of these taxa. Gamonts in association can be used to diagnose populations of *B. cubensis* from other known species, but differences are much more clearly demonstrated in correlating characters observed in gametocysts and oocysts.

Blabericola cubensis is readily distinguished from *B. haasi*, *B. migrator*, and *B. princisi* by significant differences in overall size and shape of gametocysts (cf. Fig. 4 with Figs. 12, 20, and 28, respectively; Fig. 40), and oocysts (cf. Figs. 6 with Figs. 14, 22, and 30, respectively; Figs. 41–43) by all metric measures observed. Gametocysts of *B. cubensis* and *B. princisi* are nearly spherical, but those of *B. haasi* and *B. migrator* are distinctly elliptoid. The gametocysts of *B. cubensis* are larger than those of *B. princisi* (ca. 457 μm and 368 μm in diameter, respectively). The oocysts of *B. cubensis* are larger than those of other described species and are readily distinguished by OLM/OW, OLM/OLI, and OLI/OW indices (Figs. 41–43).

***Blabericola haasi* (Geus, 1969) Clopton, 2009**

(= *Leidyana haasi* Clopton and Hays, 2006;
= *Gregarina haasi* Geus, 1969)
(Figs. 12–19)

Trophozoite (Fig. 15): Young trophozoites solitary, extracellular forms attached to host ventricular epithelium. Holdfast an orbicular epimerite without diamerite. Protomerite dolioform to shallowly dolioform, markedly constricted at protomerite-deutomerite septum. Deutomerite obovoid. Nucleus orbicular with nearly orbicular, smooth-margined, concentric karyosome.

Association (Figs. 16–19): Presyzygial, gamontic; gamonts anisomorphic due to structures involved in association interface; association interface a shallow interlock, posterior end of primite's deutomerite embedded in shallow torus formed from anterior membranes of satellite's protomerite. Measurements taken from mature gamonts in association. Indices: PTL/STL 1.08 (0.93–1.28, ±0.08, 30), PPL/SPL 1.67 (0.98–2.24, ±0.31, 30), PPWM/SPWM 0.99 (0.79–1.29, ±0.12, 30), PDL/SDL 0.98 (0.78–1.20, ±0.10, 30), PDWM/SDWM 1.05 (0.82–1.40, ±0.13, 30), PDWE/SDWE 1.04 (0.80–1.38, ±0.14, 30).

Primite: Observations and data taken from mature primites in association. Epimerite absent; protomerite variable with size, ranging from deeply deltoid or broadly pyriform in smaller specimens to finely ovoid or deltoid in larger specimens; PL 73.1 (55.1–89.9, ±8.99, 30), PWE 58.9 (44.3–76.5, ±7.89, 30), PWM 65.2 (48.9–86.5, ±10.00, 30), PLAM 49.6 (30.7–68.7, ±10.71, 30), PLPM 23.1 (5.1–51.7, ±10.31, 30), PDSW 63.2 (48.3–80.8, ±8.74, 30), PL/PWE 1.26 (0.80–1.63, ±0.23, 30), PL/PWM 1.15 (0.71–1.52, ±0.22, 30), PL/PDSW 1.18 (0.73–1.47, ±0.20, 30), PLAM/PL 0.68 (0.39–0.91, ±0.13, 30), PLAM/PLPM 2.79 (0.61–10.09, ±1.90, 30), PWM/PWE 1.11 (0.97–1.26, ±0.07, 30). Deutomerite usually obpanduriform to narrowly obpanduriform, becoming elliptoid in largest specimens; DL 244.5 (220.2–270.9, ±14.07, 30), DWE 85.6 (63.8–128.0, ±18.23, 30), DWM 92.5 (70.6–134.8, ±18.66, 30), DLAM 113.9 (13.3–197.2, ±62.44, 30), DLPM 131.3 (54.9–237.7, ±62.94, 30), DL/DWE 2.97 (1.89–3.94, ±0.57, 30), DL/DWM 2.73 (1.73–3.78, ±0.51, 30), DLAM/DL 0.47 (0.05–0.78, ±0.25, 30), DLAM/DLPM 1.40 (0.06–3.30, ±1.19, 30), DWM/DWE 1.09 (0.99–1.53, ±0.09, 30), PTL 316.5 (284.1–342.1, ±14.82, 30). Indices: PTL/PL 4.39 (3.65–5.90, ±0.53, 30), PTL/PWM 4.97 (3.75–6.89, ±0.84, 30), PTL/PWE 5.47 (4.27–7.64, ±0.80, 30), DL/PL 3.41 (2.68–4.92, ±0.54, 30), PTL/DL 1.30 (1.19–1.37, ±0.04, 30), PTL/DWM 3.54 (2.29–4.77, ±0.65, 30), PTL/DWE 3.83 (2.49–4.96, ±0.71, 30), DWM/PWM 1.42 (1.15–1.64, ±0.13, 30), DWE/PWE 1.09 (0.99–1.53, ±0.09, 30). Nucleus nearly orbicular with single, concentric orbicular karyosome; NL 27.9 (20.4–36.4, ±3.81, 30), NW 24.7 (12.3–36.3, ±5.43, 30), NDS 61.2 (8.6–172.0, ±53.84, 30), KD 12.6 (7.4–17.9, ±2.53, 30), NL/NW 1.17 (1.00–2.32, ±0.26, 30), NDS/NL 2.32 (0.31–7.27, ±2.17, 30), DL/NDS 8.57 (1.42–25.89, ±7.32, 30), NL/KD 2.28 (1.66–3.83, ±0.46, 30).

Satellite: Observations and data taken from mature satellites in association. Protomerite compressed anteriorly by association interface, very shallowly ovoid to ovoid, anterior membranes forming toroidal margin at association interface; PSSW 48.0 (34.0–82.8, ±10.08, 30), PL 44.4 (33.7–56.0, ±4.97, 30), PWE 58.8 (41.0–85.0, ±9.60, 30), PWM 66.4 (48.7–87.6, ±9.16, 30), PLAM 30.1 (17.4–38.2, ±5.54, 30), PLPM 13.7 (7.3–22.6, ±3.87, 30), PDSW 65.8 (48.9–84.0, ±8.90, 30), PL/PWE 0.78 (0.40–1.07, ±0.16, 30), PL/PWM 0.68 (0.38–0.94, ±0.13, 30), PL/PDSW 0.69 (0.40–0.96, ±0.13, 30), PLAM/PL 0.68 (0.48–0.84, ±0.10, 30), PLAM/PLPM 2.43 (0.95–4.45, ±0.94, 30), PWM/PWE 1.13 (1.03–1.28, ±0.06, 30). Deutomerite narrowly ovoid to ovoid; DL 252.5 (208.3–313.4, ±23.26, 30), DWE 82.7 (55.9–111.6, ±14.45, 30), DWM 88.7 (60.5–125.6, ±16.18, 30), DLAM 59.8 (31.3–152.5, ±25.24, 30), DLPM 191.8 (97.0–248.1, ±34.41, 30), DL/DWE 3.12 (2.37–4.05, ±0.48, 30), DL/DWM 2.91 (2.13–3.82, ±0.44, 30), DLAM/DL 0.24 (0.13–0.61, ±0.11, 30), DLAM/DLPM 0.35 (0.15–1.57, ±0.28, 30), DWM/DWE 1.07 (0.98–1.21, ±0.05, 30), STL 295.6 (250.2–349.0, ±23.78, 30). Indices: STL/PL 6.74 (5.21–9.19, ±0.92, 30), STL/PWM 4.52 (3.50–6.09, ±0.58, 30), STL/PWE 5.14 (3.61–7.18, ±0.82, 30), DL/PL 5.77 (4.31–8.25, ±0.89, 30), STL/DL 1.17 (1.11–1.22, ±0.03, 30), STL/DWM 3.41 (2.44–4.40, ±0.52, 30), STL/DWE 3.66 (2.75–4.72, ±0.57, 30), DWM/PWM 1.33 (1.16–1.62, ±0.12, 30), DWE/PWE 1.41 (1.20–1.76, ±0.13, 30). Nucleus nearly orbicular with single, nearly concentric orbicular karyosome; NL 26.7 (22.4–34.9, ±2.90, 30), NW 23.6 (17.1–29.9, ±3.69, 30), NDS 67.2 (14.6–217.8, ±56.91, 30), KD 12.0 (7.7–18.2, ±2.41, 30), NL/

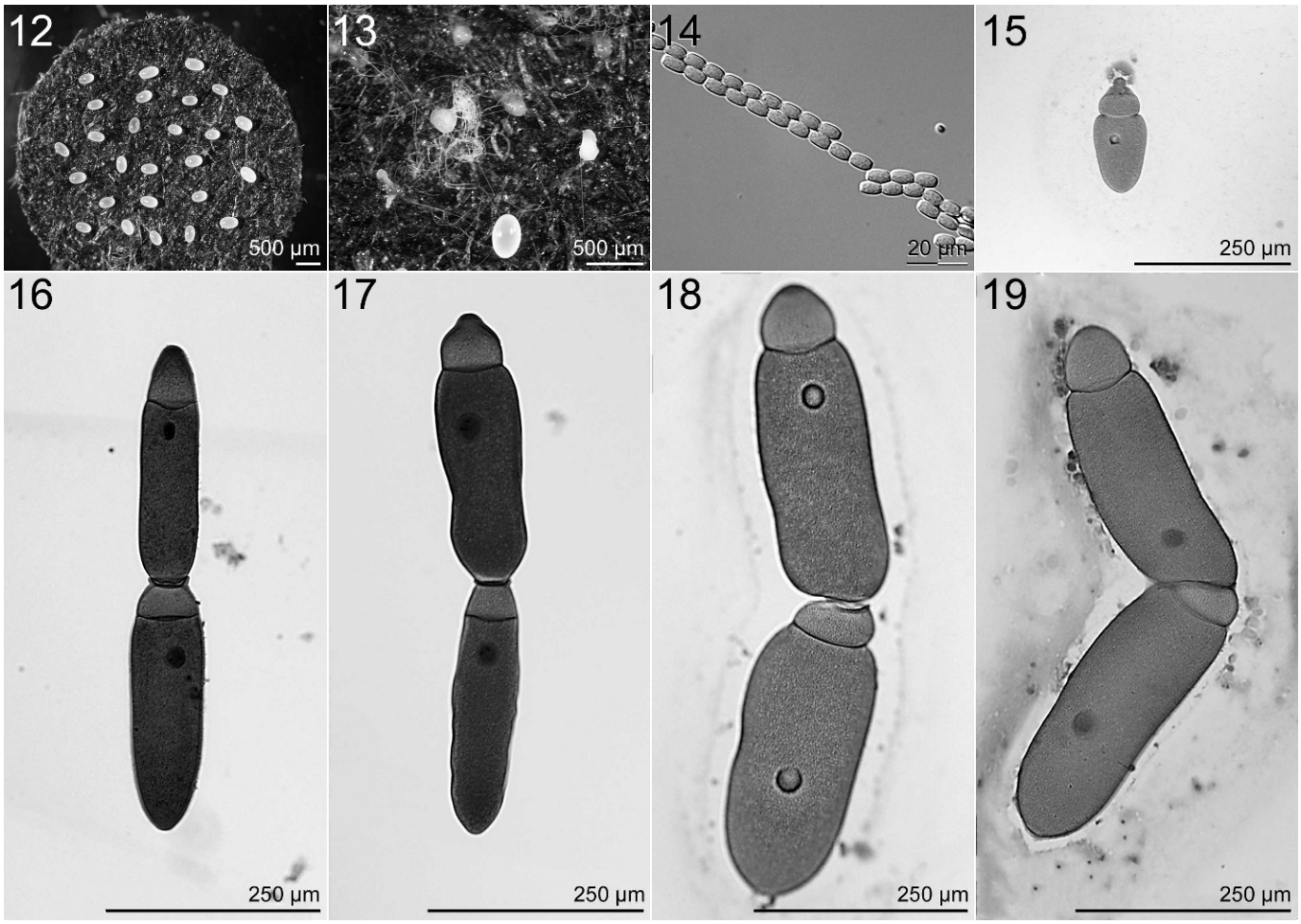

FIGURES 12–19. *Blabericola haasi*. (**12**) Gametocysts. (**13**) Monete oocyst chains dehisced from mature gametocysts. (**14**) Oocysts. (**15**) Solitary trophozoite with epimerite. (**16**–**19**) Variation in typical mature associations.

NW 1.15 (1.00–1.62, ±0.15, 30), NDS/NL 2.54 (0.57–7.94, ±2.16, 30), DL/NDS 6.87 (1.29–16.24, ±4.83, 30), NL/KD 2.29 (1.69–3.60, ±0.42, 30).

Gametocysts (Figs. 12–13): White, opaque, irregularly elliptoid, length 274.7 (263.1–286.0, ±6.66, 30), width 180.9 (166.2–193.1, ±7.68, 30), GL/GW 1.50 (1.40–1.62, ±0.06, 30). Gametocysts collected and stored under moist conditions dehisced within 24–36 hr, releasing oocysts in monete chains by extrusion.

Oocysts (Figs. 13–14): Dolioform with outline smoothing to incorporate terminal polar plates, single oocyst residuum simple, smooth, orbicular, nearly terminal; OLM 8.0 (7.8–8.2, ±0.12, 30), OLI 6.6 (6.3–6.9, ±0.15, 30), OW 4.8 (4.6–5.0, ±0.13, 30), PPW 2.6 (2.2–3.0, ±0.19, 30), PPL 0.7 (0.4–1.1, ±0.17, 30), ResDia 1.1 (0.8–1.5, ±0.16, 30), OLM/OLI 1.20 (1.20–1.30, ±0.03, 30), OLM/OW 1.70 (1.60–1.80, ±0.05, 30), OLI/OW 1.40 (1.30–1.50, ±0.05, 30), PPW/PPL 3.80 (2.30–5.80, ±0.91, 30), OW/PPW 1.80 (1.60–2.20, ±0.13, 30), OLM/PPL 11.60 (7.10–18.70, ±2.63, 30), OLM/ResDia 7.20 (5.30–9.80, ±1.07, 30), OW/ResDia 4.30 (3.40–6.00, ±0.66, 30).

Taxonomic summary

Type host: Nauphoeta cinerea (Olivier, 1789) (Dictyoptera: Blattaria: Blaberidae: Oxyhalinae: Nauphoetini).

Type locality: Ndanda Abbey, Ndanda, Tanzania.

Type specimens: Neotype (hapantotype) HWML no. 48313, Harold W. Manter Laboratory for Parasitology (HWML), Division of Parasitology, University of Nebraska State Museum, Lincoln, Nebraska.

Site of infection: Trophozoites were collected from ventricular cecae and post-intercecal region. Associations were collected from the anterior mesenteron. Gametocysts were collected from host feces.

Prevalence: Prevalence in colony approaches 100%.

Records: Laboratory cultures, nymphs, and adults, Peru State College, Peru, Nebraska.

Specimens deposited: The voucher slide series for this redescription is deposited in the Harold W. Manter Laboratory for Parasitology (HWML), Division of Parasitology, University of Nebraska State Museum, Lincoln, Nebraska and comprises 42 hapantotype slides containing multiple trophozoites, gamonts, and associations accessioned as HWML100046. Many of these slides also include specimens of *Protomagalhaensia wolfi* (Geus, 1969) Clopton and Hays, 2006, which commonly co-occurs with *B. haasi* in *N. cinerea*.

Remarks

Blabericola haasi is distinguished from other known species of *Blabericola* by significant differences in overall size and shape of gamonts in association (cf. Figs. 16–19 with Figs. 8–11, Figs. 24–27, and Figs. 32–35; Figs. 36–39), by all metric measures observed except PriPLPM and PriDLAM, which were not significantly different from those of *B. migrator* or *B. princisi*; PriPDSW, SatPLAM, SatPLPM, and SatTL, which were not significantly different from those of *B. migrator*; and PriNDS and SatNW, which were not significantly different from those of *B. princisi*. In general, gamonts of *B. haasi* are roughly half the size of those of other blabericolids and are notably smaller by all significant metrics. Centroid clustering diagrams of differential gamont metrics (Figs. 36–39) readily demonstrate these differences.

Blabericola haasi is readily distinguished from *B. cubensis*, *B. migrator*, and *B. princisi* by significant differences in overall size and shape of

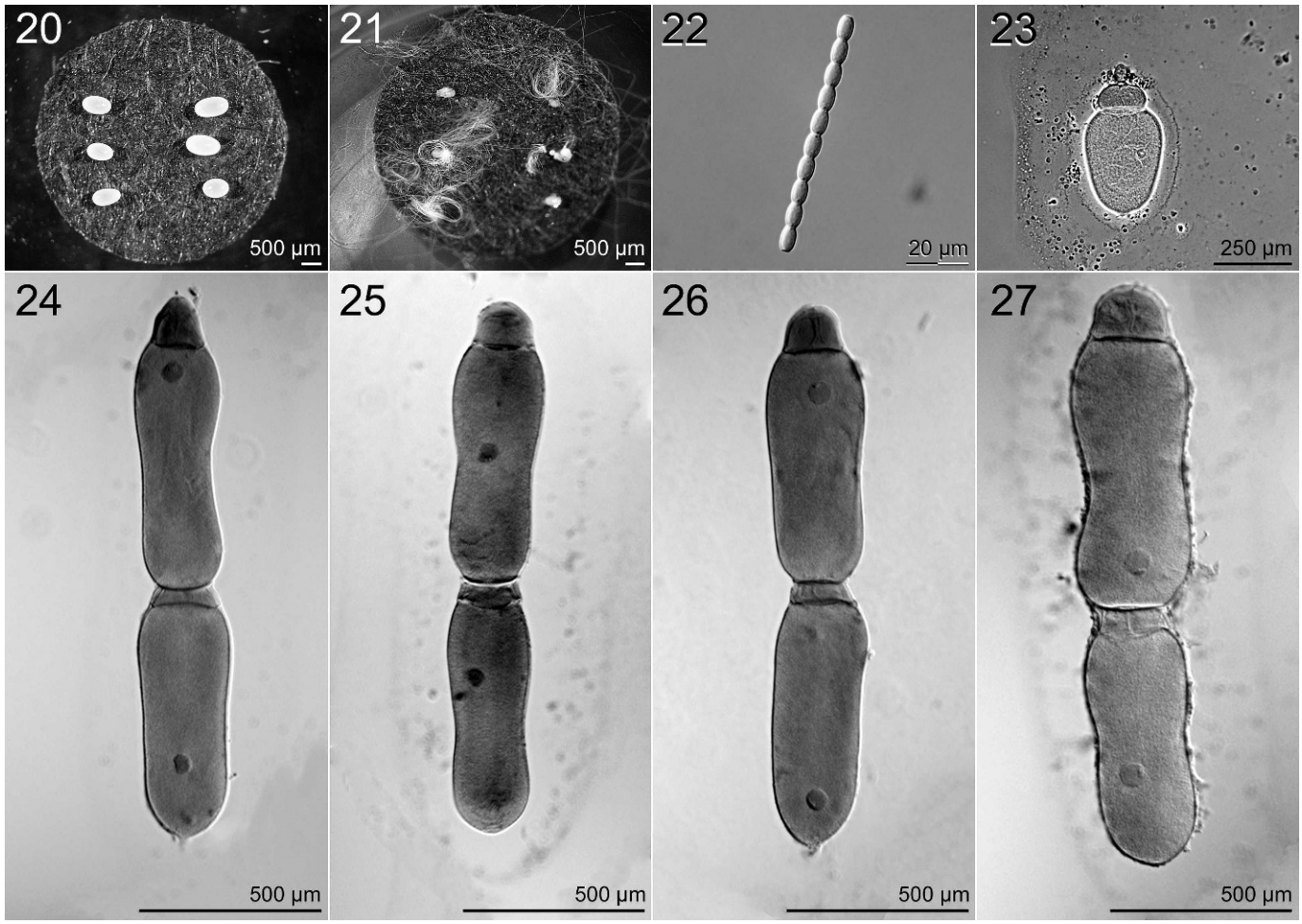

FIGURES 20–27. *Blabericola migrator*. (**20**) Gametocysts. (**21**) Monete oocyst chains dehisced from mature gametocysts. (**22**) Oocysts. (**23**) Solitary trophozoite with epimerite. (**24**–**27**) Variation in typical mature associations.

gametocysts (cf. Fig. 12 with Figs. 4, 20, and 28, respectively; Fig. 40), and oocysts (cf. Figs. 14 with Figs. 6, 22, and 30, respectively; Figs. 41–43) by all metric measures, although the GL/GW index of *B. haasi* gametocysts is not significantly different from that of *B. migrator*. Although similarly elliptoid in shape, the gametocysts of *B. haasi* are less than half the size of the gametocysts of *B. migrator* (ca. 275 µm × 181 µm vs. 700 µm × 453 µm, respectively). Gametocysts of *B. cubensis* and *B. princisi* are nearly spherical and, thus, readily distinguishable from those of *B. haasi*. The oocysts of *B. haasi* are smaller than those of other described species but most similar in size to those of *B. migrator*; nonetheless, they are readily distinguished by OLM/OLI and OLI/OW indices (Figs. 41–43).

Blabericola migrator **(Clopton, 1995) Clopton, 2009**

(= *Leidyana migrator* Clopton, 1995)

(Figs. 20–27)

Trophozoite (Fig. 23): Young trophozoites solitary, extracellular forms attached to host ventricular epithelium. Holdfast an orbicular epimerite without diamerite. Protomerite dolioform to shallowly dolioform, markedly constricted at protomerite-deutomerite septum. Deutomerite obovoid. Nucleus orbicular with nearly orbicular, smooth-margined, concentric karyosome.

Association (Figs. 24–27): Presyzygial, gamontic; gamonts anisomorphic due to structures involved in association interface; association interface a shallow interlock, posterior end of primite's deutomerite embedded in shallow torus formed from anterior membranes of satellite's protomerite. Measurements taken from mature gamonts in association. Indices: PTL/STL 1.16 (1.05–1.33, ±0.08, 30), PPL/SPL 2.04 (1.47–3.16, ±0.45, 30), PPWM/SPWM 0.95 (0.74–1.20, ±0.12, 30), PDL/SDL 1.07 (0.92–1.20, ±0.07, 30), PDWM/SDWM 0.97 (0.72–1.24, ±0.11, 30), PDWE/SDWE 0.95 (0.69–1.45, ±0.15, 30).

Primite: Observations and data taken from mature primites in association. Epimerite absent; protomerite very shallowly to very broadly ovoid; PL 133.0 (100.0–166.7, ±13.56, 30), PWE 150.7 (122.0–174.7, ±16.45, 30), PWM 171.5 (143.0–201.7, ±17.40, 30), PLAM 111.0 (67.9–137.3, ±14.30, 30), PLPM 22.8 (2.6–61.9, ±13.19, 30), PDSW 174.1 (141.4–210.3, ±20.01, 30), PL/PWE 0.89 (0.68–1.09, ±0.12, 30), PL/PWM 0.78 (0.57–0.93, ±0.10, 30), PL/PDSW 0.77 (0.56–0.92, ±0.10, 30), PLAM/PL 0.84 (0.53–1.04, ±0.11, 30), PLAM/PLPM 7.93 (1.10–40.46, ±8.11, 30), PWM/PWE 1.14 (1.05–1.23, ±0.05, 30). Deutomerite narrowly obpanduriform to obpanduriform; DL 623.0 (479.2–709.0, ±69.43, 30), DWE 215.8 (182.8–285.2, ±25.75, 30), DWM 252.8 (204.8–299.0, ±25.85, 30), DLAM 125.6 (79.6–156.4, ±23.10, 30), DLPM 495.4 (366.3–596.5, ±70.61, 30), DL/DWE 2.92 (1.87–3.61, ±0.43, 30), DL/DWM 2.48 (1.78–2.90, ±0.29, 30), DLAM/DL 0.20 (0.13–0.29, ±0.04, 30), DLAM/DLPM 0.26 (0.14–0.42, ±0.07, 30), DWM/DWE 1.18 (1.03–1.33, ±0.08, 30), PTL 755.1 (609.1–845.1, ±71.87, 30). Indices: PTL/PL 5.73 (4.50–7.82, ±0.79, 30), PTL/PWM 4.42 (3.60–5.48, ±0.44, 30), PTL/PWE 5.05 (3.78–6.44, ±0.59, 30), DL/PL 4.74 (3.50–6.88, ±0.79, 30), PTL/DL 1.21 (1.14–1.29, ±0.03, 30), PTL/DWM 3.01 (2.29–3.48, ±0.32, 30), PTL/DWE 3.54 (2.40–4.36, ±0.47, 30), DWM/PWM 1.48 (1.29–1.75, ±0.11, 30), DWE/PWE 1.18 (1.03–1.33, ±0.08, 30). Nucleus nearly orbicular, slightly irregular in outline with single, eccentric orbicular karyosome; NL 64.0 (53.1–79.6, ±7.61, 30), NW 58.3 (47.2–75.0, ±6.73, 30), NDS 143.0 (25.6–578.8, ±155.18, 30), KD 26.3 (17.9–34.4, ±4.07, 30), NL/NW 1.10 (1.01–1.31, ±0.08, 30), NDS/NL 2.24 (0.38–8.26, ±2.33, 30), DL/NDS 8.37 (1.22–27.56, ±5.84, 30), NL/KD 2.48 (1.82–3.86, ±0.42, 30).

Satellite: Observations and data taken from mature satellites in association. Protomerite compressed anteriorly by association interface, depressed oblong to oblong, anterior membranes forming toroidal margin at association interface; PSSW 151.6 (95.6–219.6, ±26.62, 30), PL 67.6 (43.4–87.5, ±11.82, 30), PWE 162.4 (115.8–223.7, ±22.46, 30), PWM 183.4 (129.9–245.4, ±25.02, 30), PLAM 47.8 (31.6–69.0, ±8.51, 30), PLPM 17.9 (3.6–31.4, ±7.41, 30), PDSW 184.3 (132.7–238.2, ±25.30, 30), PL/PWE 0.43 (0.24–0.74, ±0.12, 30), PL/PWM 0.38 (0.21–0.66, ±0.10, 30), PL/PDSW 0.38 (0.22–0.65, ±0.10, 30), PLAM/PL 0.72 (0.47–0.96, ±0.12, 30), PLAM/PLPM 3.41 (1.08–12.01, ±2.22, 30), PWM/PWE 1.13 (1.05–1.27, ±0.04, 30). Deutomerite obpanduriform to irregularly lomentiform; DL 585.8 (466.1–684.0, ±67.20, 30), DWE 230.8 (172.9–309.4, ±37.63, 30), DWM 262.9 (198.9–339.2, ±37.13, 30), DLAM 119.9 (82.7–169.8, ±20.61, 30), DLPM 465.1 (345.0–562.4, ±60.46, 30), DL/DWE 2.58 (1.84–3.30, ±0.39, 30), DL/DWM 2.25 (1.66–2.86, ±0.29, 30), DLAM/DL 0.21 (0.16–0.28, ±0.03, 30), DLAM/DLPM 0.26 (0.19–0.38, ±0.06, 30), DWM/DWE 1.14 (1.02–1.30, ±0.07, 30), STL 651.0 (543.2–760.4, ±64.45, 30). Indices: STL/PL 9.97 (6.51–15.77, ±2.25, 30), STL/PWM 3.59 (2.73–4.31, ±0.41, 30), STL/PWE 4.06 (2.99–4.83, ±0.50, 30), DL/PL 9.01 (5.46–14.71, ±2.23, 30), STL/DL 1.11 (1.07–1.19, ±0.03, 30), STL/DWM 2.51 (1.88–3.08, ±0.31, 30), STL/DWE 2.87 (2.09–3.56, ±0.42, 30), DWM/PWM 1.44 (1.22–1.75, ±0.13, 30), DWE/PWE 1.43 (1.18–1.84, ±0.17, 30). Nucleus nearly orbicular, slightly irregular in outline with single, eccentric orbicular karyosome; NL 63.9 (55.4–86.2, ±6.50, 30), NW 69.7 (45.9–416.9, ±65.77, 30), NDS 202.8 (31.9–509.0, ±141.68, 30), KD 27.6 (18.1–39.1, ±4.40, 30), NL/NW 1.08 (0.14–1.41, ±0.20, 30), NDS/NL 3.14 (0.53–8.34, ±2.18, 30), DL/NDS 4.96 (1.30–14.62, ±4.00, 30), NL/KD 2.35 (1.81–3.61, ±0.36, 30).

Gametocysts (Figs. 20–21): White, opaque, irregularly elliptoid, length 700.2 (658.0–739.4, ±26.69, 30), width 453.0 (433.2–473.2, ±11.13, 30), GL/GW 1.50 (1.40–1.70, ±0.06, 30). Gametocysts collected and stored under moist conditions dehisced within 24–36 hr, releasing oocysts in monete chains by extrusion.

Oocysts (Figs. 21–22): Dolioform with outline smoothing to incorporate terminal polar plates, single oocyst residuum simple, smooth, orbicular, nearly terminal; OLM 7.9 (7.8–8.0, ±0.08, 30), OLI 7.2 (7.0–7.4, ±0.12, 30), OW 4.7 (4.6–4.8, ±0.08, 30), PPW 2.2 (2.0–2.5, ±0.14, 30), PPL 0.4 (0.3–0.5, ±0.06, 30), ResDia 0.9 (0.8–1.1, ±0.08, 30), OLM/OLI 1.10 (1.10–1.10, ±0.01, 30), OLM/OW 1.70 (1.60–1.80, ±0.03, 30), OLI/OW 1.50 (1.50–1.60, ±0.03, 30), PPW/PPL 5.90 (4.40–8.30, ±0.87, 30), OW/PPW 2.10 (1.90–2.30, ±0.12, 30), OLM/PPL 21.00 (15.30–28.10, ±3.08, 30), OLM/ResDia 8.80 (7.30–10.10, ±0.79, 30), OW/ResDia 5.20 (4.40–5.90, ±0.46, 30).

Taxonomic summary

Type host: Gromphadorhina portentosa Brunner von Wattenwyl, 1865 (Dictyoptera: Blattaria: Blaberidae: Oxyhaloinae: Gromphadorhini), nymphs and adults.

Type locality: Laboratory cultures, Department of Entomology, Texas A&M University, College Station, Texas.

Type specimens: Full type series, holotype, and paratype slides, USNPC no. 84555–84556, U. S. National Parasite Collection, USDA–Beltsville Agricultural Research Center, Beltsville, Maryland; 6 paratype slides HMWL no. 38218 and 38219, Harold W. Manter Laboratory for Parasitology (HWML), Division of Parasitology, University of Nebraska State Museum, Lincoln, Nebraska.

Site of infection: Trophozoites were collected from ventricular cecae and post-intercecal region. Associations were collected from the anterior mesenteron. Gametocysts were collected from host feces.

Prevalence: Prevalence in colony approaches 100%.

Records: Laboratory cultures, nymphs, and adults, Peru State College, Peru, Nebraska.

Specimens deposited: The voucher slide series for this redescription is deposited in the Harold W. Manter Laboratory for Parasitology (HWML), Division of Parasitology, University of Nebraska State Museum, Lincoln, Nebraska and comprises 31 hapantotype slides containing multiple trophozoites, gamonts, and associations accessioned as HWML100047.

Remarks

Blabericola migrator is distinguished from other known species of *Blabericola* by significant differences in overall size and shape of gamonts in association (cf. Figs. 24–27 with Figs. 8–11, Figs. 16–19, and Figs. 32–35; Figs. 36–39), by all metric measures observed except PriNDS, which was not significantly different from that of *B. cubensis*; PriNDS, which was not significantly different from that of *B. princisi*; PriPDSW, SatPLAM, SatPLPM, and SatTL, which were not significantly different from those of *B. haasi*; SatPL, SatPLAM, and SatNW, which were not significantly different from those of *B. cubensis* or B. *princisi*; and PriPLPM and PriDLAM, which were not significantly different from those of *B. haasi* or *B. princisi.* In general, gamonts of *B. migrator* are notably larger than those of other blabericolids by all significant metrics. Centroid clustering diagrams of differential gamont metrics (Figs. 36–39) readily demonstrate these differences.

Blabericola migrator is readily distinguished from *B. cubensis*, *B. haasi*, and *B. princisi* by significant differences in overall size and shape of gametocysts (cf. Fig. 20 with Figs. 4, 12, and 28, respectively; Fig. 40), and oocysts (cf. Figs. 22 with Figs. 6, 14, and 30, respectively; Figs. 41–43) by all metric measures, although the GL/GW index of *B. migrator* gametocysts is not significantly different from that of *B. haasi.* Although similarly elliptoid in shape, the gametocysts of *B. haasi* are less than half the size of the gametocysts of *B. migrator* (ca. 275 μm × 181 μm vs. 700 μm × 453 μm, respectively). Gametocysts of *B. cubensis* and *B. princisi* are nearly spherical and, thus, readily distinguished from those of *B. migrator*. Although the gamonts and gametocysts of *B. migrator* are notably larger than those of other blabericolids, the oocysts of *B. migrator* are smaller than those of *B. cubensis* and *B. princisi* and most similar in size to those of *B. migrator*; nonetheless, they are readily distinguished by OLM/OLI and OLI/OW indices (Figs. 41–43).

Blabericola princisi **(Peregrine, 1970) Clopton, 2009**

(= *Gregarina princisi* Peregrine, 1970)

(Figs. 28–35)

Trophozoite (Fig. 31): Young trophozoites solitary, extracellular forms attached to host ventricular epithelium. Holdfast a gladiate epimerite without diamerite. Protomerite broadly ovoid, markedly constricted at protomerite-deutomerite septum. Deutomerite narrowly obovoid. Nucleus orbicular with nearly orbicular, smooth-margined, eccentric karyosome.

Association (Figs. 32–35): Presyzygial, gamontic; gamonts anisomorphic due to structures involved in association interface; association interface a shallow interlock, posterior end of primite's deutomerite embedded in shallow torus formed from anterior membranes of satellite's protomerite. Measurements taken from mature gamonts in association. Indices: PTL/STL 1.06 (0.91–1.30, ±0.11, 30), PPL/SPL 1.44 (1.09–2.40, ±0.28, 30), PPWM/SPWM 1.10 (0.89–1.30, ±0.12, 30), PDL/SDL 0.99 (0.84–1.24, ±0.11, 30), PDWM/SDWM 1.01 (0.71–1.25, ±0.14, 30), PDWE/SDWE 0.97 (0.67–1.19, ±0.15, 30).

Primite: Observations and data taken from mature primites in association. Epimerite absent; protomerite ovoid to very broadly ovoid; PL 96.6 (77.3–128.6, ±13.10, 30), PWE 96.8 (73.6–138.8, ±14.64, 30), PWM 111.0 (91.1–145.7, ±14.12, 30), PLAM 68.2 (42.4–101.9, ±14.96, 30), PLPM 28.5 (17.1–48.6, ±8.62, 30), PDSW 110.0 (90.4–142.5, ±13.37, 30), PL/PWE 1.01 (0.67–1.39, ±0.17, 30), PL/PWM 0.88 (0.62–1.09, ±0.11, 30), PL/PDSW 0.88 (0.64–1.08, ±0.11, 30), PLAM/PL 0.70 (0.46–0.85, ±0.09, 30), PLAM/PLPM 2.67 (0.91–5.47, ±1.13, 30), PWM/PWE 1.15 (0.98–1.30, ±0.08, 30). Deutomerite narrowly obpanduriform to obpanduriform; DL 447.7 (398.8–495.3, ±24.17, 30), DWE 136.3 (92.1–226.9, ±31.89, 30), DWM 152.2 (107.8–231.6, ±30.27, 30), DLAM 87.5 (34.7–328.0, ±62.13, 30), DLPM 360.1 (147.3–428.5, ±66.38, 30), DL/DWE 3.44 (2.03–5.08, ±0.72, 30), DL/DWM 3.04 (1.99–4.34, ±0.54, 30), DLAM/DL 0.20 (0.08–0.69, ±0.14, 30), DLAM/DLPM 0.31 (0.08–2.23, ±0.44, 30), DWM/DWE 1.13 (1.00–1.28, ±0.07, 30), PTL 543.4 (483.4–601.8, ±33.03, 30). Indices: PTL/PL 5.68 (4.68–6.45, ±0.52, 30), PTL/PWM 4.95 (3.92–6.04, ±0.55, 30), PTL/PWE 5.71 (4.15–7.35, ±0.79, 30), DL/PL 4.69 (3.67–5.46, ±0.52, 30), PTL/DL 1.21 (1.18–1.28, ±0.03, 30), PTL/DWM 3.68 (2.40–5.13, ±0.63, 30), PTL/DWE 4.17 (2.45–6.01, ±0.85, 30), DWM/PWM 1.37 (1.06–1.93, ±0.19, 30), DWE/PWE 1.13 (1.00–1.28, ±0.07, 30). Nucleus nearly orbicular with single, eccentric orbicular karyosome; NL 45.3 (32.7–63.1, ±6.10, 30), NW 40.8 (30.6–62.2, ±6.13, 30), NDS 70.1 (9.3–369.7, ±76.76, 30), KD 16.2 (11.5–21.1, ±2.69, 30), NL/NW 1.12 (1.00–1.37, ±0.11, 30), NDS/NL 1.54 (0.15–8.09, ±1.65, 30), DL/NDS 12.73 (1.19–48.51, ±10.09, 30), NL/KD 2.87 (2.06–4.65, ±0.57, 30).

Satellite: Observations and data taken from mature satellites in association. Protomerite compressed anteriorly by association interface, shallowly dolioform to very shallowly ovoid, anterior membranes forming

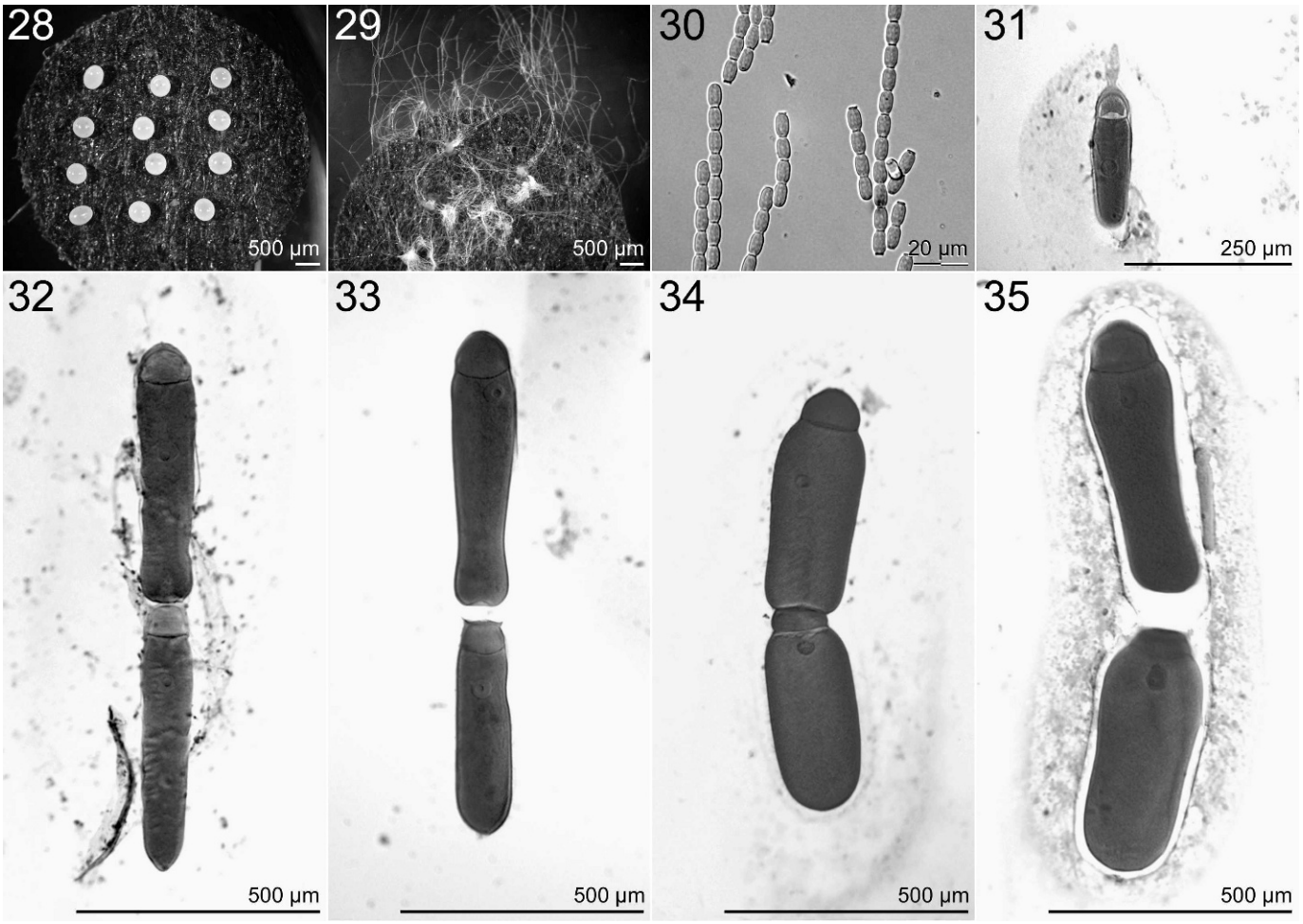

FIGURES 28–35. *Blabericola princisi*. (**28**) Gametocysts. (**29**) Monete oocyst chains dehisced from mature gametocysts. (**30**) Oocysts. (**31**) Solitary trophozoite with epimerite. (**32**–**35**) Variation in typical mature associations.

toroidal margin at association interface; PSSW 82.9 (61.3–113.4, ±12.28, 30), PL 68.0 (45.2–99.4, ±9.81, 30), PWE 93.1 (72.5–111.2, ±11.63, 30), PWM 101.8 (77.5–129.5, ±13.27, 30), PLAM 43.2 (28.7–57.8, ±7.78, 30), PLPM 24.0 (9.1–46.3, ±9.90, 30), PDSW 102.0 (77.7–131.1, ±13.43, 30), PL/PWE 0.74 (0.41–1.01, ±0.14, 30), PL/PWM 0.68 (0.36–0.94, ±0.14, 30), PL/PDSW 0.68 (0.36–0.94, ±0.14, 30), PLAM/PL 0.64 (0.43–0.84, ±0.12, 30), PLAM/PLPM 2.17 (0.74–4.69, ±1.04, 30), PWM/PWE 1.09 (0.98–1.24, ±0.06, 30). Deutomerite narrowly obovoid to obpanduriform; DL 455.5 (353.0–527.8, ±51.41, 30), DWE 142.9 (89.4–207.6, ±34.97, 30), DWM 153.6 (107.6–224.1, ±35.86, 30), DLAM 117.3 (50.1–322.8, ±63.85, 30), DLPM 335.8 (132.3–428.6, ±75.31, 30), DL/DWE 3.38 (2.04–5.28, ±0.93, 30), DL/DWM 3.12 (2.01–4.86, ±0.82, 30), DLAM/DL 0.26 (0.11–0.67, ±0.14, 30), DLAM/DLPM 0.43 (0.14–2.08, ±0.45, 30), DWM/DWE 1.08 (0.97–1.22, ±0.07, 30), STL 517.9 (402.3–594.9, ±55.32, 30). Indices: STL/PL 7.72 (5.59–11.11, ±1.15, 30), STL/PWM 5.16 (3.88–6.83, ±0.79, 30), STL/PWE 5.64 (3.92–7.48, ±0.88, 30), DL/PL 6.80 (5.03–10.07, ±1.09, 30), STL/DL 1.14 (1.08–1.18, ±0.02, 30), STL/DWM 3.56 (2.29–5.42, ±0.93, 30), STL/DWE 3.85 (2.32–6.03, ±1.06, 30), DWM/PWM 1.50 (1.06–1.96, ±0.22, 30), DWE/PWE 1.52 (1.16–2.14, ±0.24, 30). Nucleus nearly orbicular with single, nearly concentric orbicular karyosome; NL 44.8 (28.5–57.7, ±6.11, 30), NW 39.1 (20.6–55.3, ±6.30, 30), NDS 125.2 (9.0–389.5, ±99.80, 30), KD 14.9 (7.7–21.3, ±3.08, 30), NL/NW 1.16 (1.00–2.01, ±0.19, 30), NDS/NL 2.87 (0.20–8.20, ±2.38, 30), DL/NDS 8.15 (1.35–55.39, ±10.24, 30), NL/KD 3.10 (2.15–4.20, ±0.55, 30).

Gametocysts (Figs. 28–29): White, opaque, irregularly orbicular to elliptoid, length 368.4 (337.6–406.1, ±20.28, 30), width 344.9 (317.1–381.5, ±19.03, 30), GL/GW 1.10 (1.00–1.10, ±0.03, 30). Gametocysts collected and stored under moist conditions dehisced within 24–36 hr, releasing oocysts in monete chains by extrusion.

Oocysts (Figs. 28–29): Dolioform with outline smoothing to incorporate terminal polar plates, single oocyst residuum simple, smooth, orbicular, nearly terminal; OLM 8.9 (8.7–9.1, ±0.10, 30), OLI 7.3 (7.1–7.5, ±0.15, 30), OW 5.1 (5.0–5.2, ±0.06, 30), PPW 2.8 (2.5–3.1, ±0.17, 30), PPL 0.8 (0.5–1.2, ±0.15, 30), ResDia 1.0 (0.8–1.2, ±0.11, 30), OLM/OLI 1.20 (1.20–1.30, ±0.03, 30), OLM/OW 1.70 (1.70–1.80, ±0.04, 30), OLI/OW 1.40 (1.40–1.50, ±0.03, 30), PPW/PPL 3.50 (2.30–5.70, ±0.79, 30), OW/PPW 1.80 (1.60–2.10, ±0.11, 30), OLM/PPL 11.00 (7.50–17.20, ±2.14, 30), OLM/ResDia 8.60 (7.30–11.50, ±0.98, 30), OW/ResDia 5.00 (4.10–6.70, ±0.57, 30).

Taxonomic summary

Type host: Blaberus boliviensis Princis, 1946 (Dictyoptera: Blattaria: Blaberidae: Blaberinae).

Type locality: Laboratory cultures, Department of Zoology, University College Cardiff (Cardiff University), Cardiff, Wales, U. K.

Types specimens: Holotype is a hapantotype slide, registration number 1970:3:3:2, The Natural History Museum, London, England, U. K.

Site of infection: Trophozoites were collected from ventricular cecae and post-intercecal region. Associations were collected from the anterior mesenteron. Gametocysts were collected from host feces.

Prevalence: Prevalence in colony approaches 100%.

Records: Laboratory cultures, nymphs, and adults, Peru State College, Peru, Nebraska.

Specimens deposited: The voucher slide series for this redescription is deposited in the Harold W. Manter Laboratory for Parasitology (HWML), Division of Parasitology, University of Nebraska State Museum, Lincoln, Nebraska and comprises 22 hapantotype slides

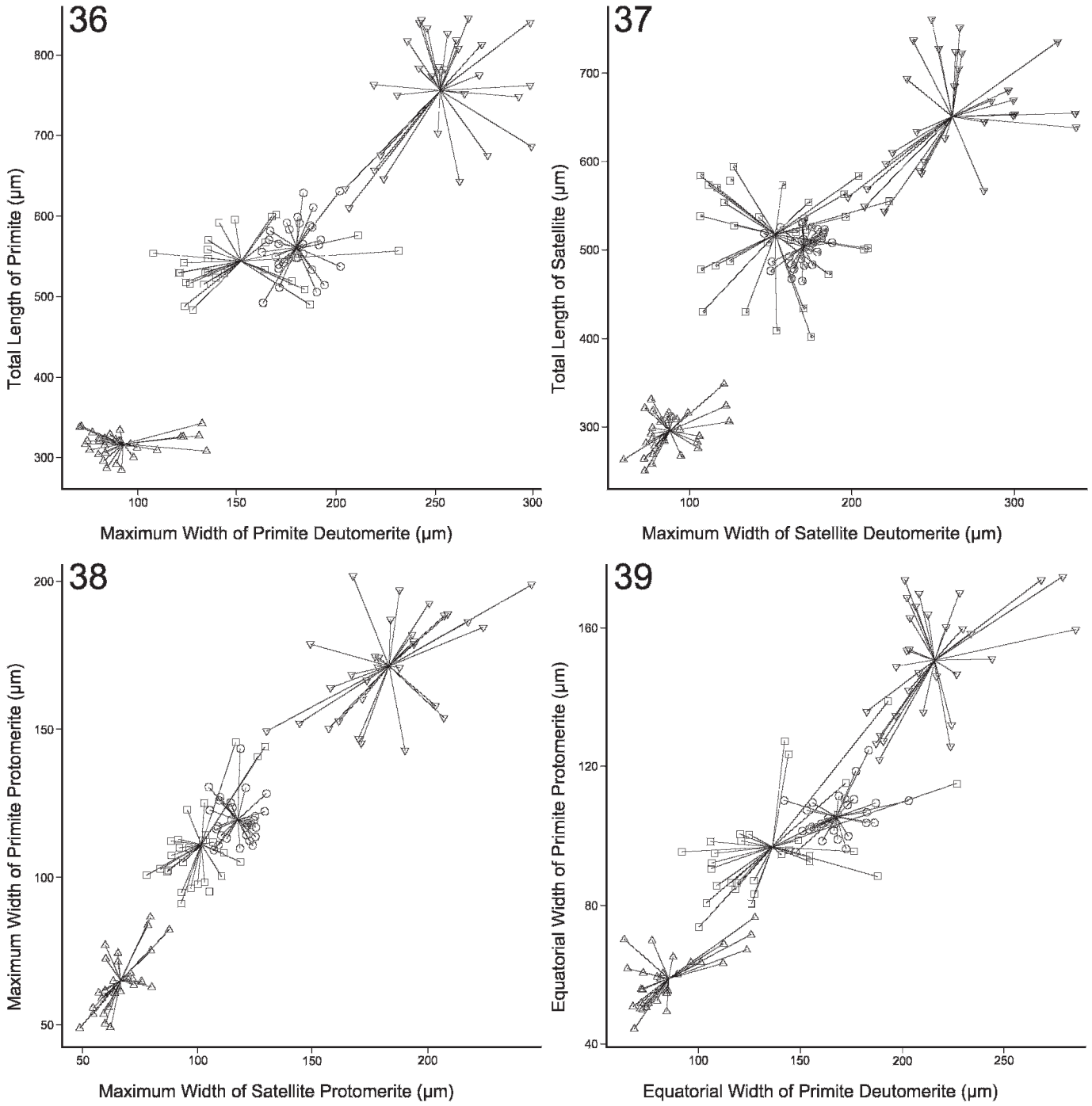

FIGURES 36–39. Centroid clustering of *Blabericola cubensis* (○), *Blabericola haasi* (△), *Blabericola migrator* (▽), and *Blabericola princisi* (□) based on differences in relative morphometric size and shape of mature gamonts in association. Centroid clusters illustrate the population variation and central morphometric tendency of each species within a 95% confidence interval (n = 30 individuals/species randomly drawn from population sample members within 2 standard deviations of the mean centroid). (**36**) Ratio of primite total length and maximum deutomerite width. (**37**) Ratio of satellite total length and maximum deutomerite width. (**38**) Ratio of primite and satellite protomerite widths. (**39**) Ratio of primite protomerite and satellite equatorial widths.

containing multiple trophozoites, gamonts, and associations accessioned as HWML100048.

Remarks

Blabericola princisi is readily distinguished from *B. haasi* and *B. migrator* by significant differences in overall size and shape of gamonts in association (cf. Figs. 32–35 with Figs. 16–19 and Figs. 24–27, respectively; Figs. 36–39) by all metric measures observed except PriPLPM, PriDLAM, PriNDS, SatPL, and SatDLAM, which were not significantly different from those of *B. migrator*. In general, gamonts of *B. princisi* are larger than those of *B. haasi* but smaller than those of *B. migrator* by all significant metrics. Gamonts of *B. princisi* are most similar to those of *B. cubensis* (cf. Figs. 32–35 with Figs. 8–11; Figs. 36–39) but exhibit

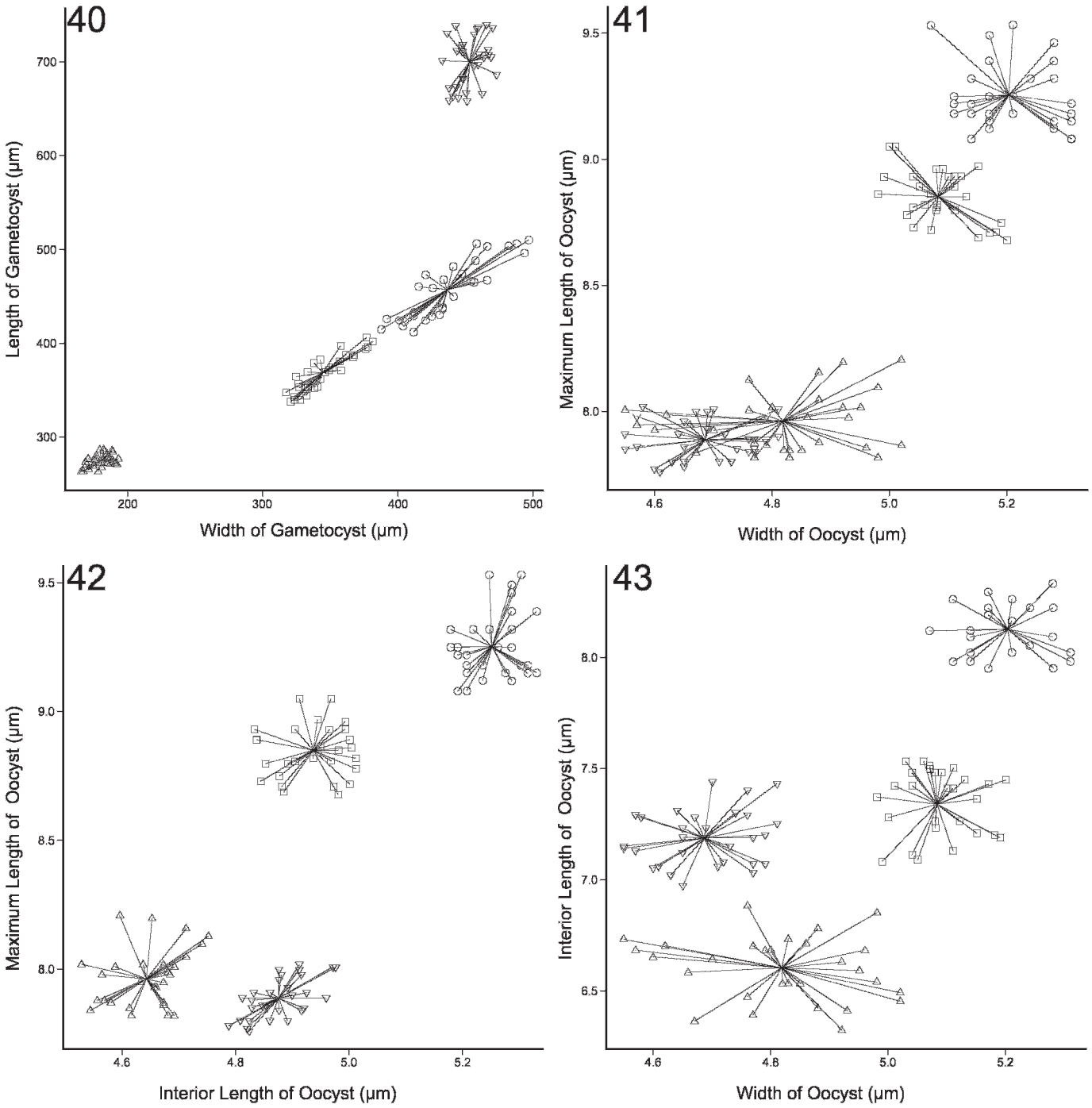

FIGURES 40–43. Centroid clustering of *Blabericola cubensis* (○), *Blabericola haasi* (△), *Blabericola migrator* (▽), and *Blabericola princisi* (□) based on differences in relative morphometric size and shape of gametocysts and oocysts. Centroid clusters illustrate the population variation and central morphometric tendency of each species within a 95% confidence interval (n = 30 individuals/species randomly drawn from population sample members within 2 standard deviations of the mean centroid). (**40**) Ratio of gametocyst length and width. (**41**) Ratio of oocyst maximum length and width. (**42**) Ratio of oocyst maximum length and interior length. (**43**) Ratio of oocyst interior length and width.

consistently and significantly smaller PriPWE, PriDWE, PriDWM, PriNL, PriNW, PriKD, PSSW, SatPWE, SatPWM, SatPDSW, SatNL, and SatKD metrics. In general, gamonts of *B. princisi* possess deutomerites that are narrower and more obviously obpanduriform than those of *B. cubensis.* The primite protomerites are elliptoid or ovoid in *B. cubensis* but deltoid in *B. princisi*. Centroid clustering diagrams of differential gamont metrics (Figs. 36–39) readily demonstrate significant differences between all 4 species while illustrating the significant metric overlap of *B. cubensis* and *B. princisi*. The toroidal margin of the primite-satellite interface formed by the anterior membranes of the satellite protomerite is much longer and more pronounced in *B. princisi* than in *B. cubensis* (cf. Figs. 32–35 and 8–11, respectively), a consistent difference also noted by Peregrine (1970) in her original descriptions of these taxa. Gamonts in association can be used to diagnose populations of *B. cubensis* from other known species, but differences are much more clearly demonstrated in correlating characters observed in gametocysts and oocysts.

Blabericola princisi is readily distinguished from *B. cubensis*, *B. haasi*, and *B. migrator* by significant differences in overall size and shape of gametocysts (cf. Fig. 28 with Figs. 4, 12, and 20, respectively; Fig. 40) and oocysts (cf. Figs. 30 with Figs. 6, 14, and 22, respectively; Figs. 41–43) by all metric measures observed. Gametocysts of *B. cubensis* and *B. princisi* are nearly spherical but those of *B. haasi* and *B. migrator* are distinctly elliptoid. The gametocysts of *B. cubensis* are larger than those of *B. princisi* (ca. 457 μm and 368 μm in diameter, respectively). The oocysts of *B. cubensis* are larger than those of *B. haasi* and *B. migrator* but smaller than those of *B. cubensis*; however, oocysts of all 4 species are readily distinguished by OLM/ OW, OLM/OLI, and OLI/OW indices (Figs. 41–43).

DISCUSSION

Any study of biodiversity begins with a definition of basic biological units, usually species, before any attempt is made to elucidate meaningful evolutionary relationships among taxa. The systematics and taxonomy of the Eugregarinorida have traditionally depended upon morphological, life cycle, and host association characters to recognize and delineate taxa in the species group. Increasing use of molecular sequence data to infer phylogeny within the group has led some authors to question the utility of established character sets and suggest that species delineation should depend on molecular sequence evidence (Rueckert and Leander, 2009; Rueckert et al., 2011). This view may reflect the often laborious effort required to collect and analyze morphological and life cycle data rather than any actual question of their utility (e.g., see Rueckert and Leander [2009] on the ''difficulty'' of using merogony as a viable character delineating *Selenidium* [Eugregarinida] and *Selenidioides* [Archigregarinida]).

Rueckert, Villette, and Leander (2011) purport to test the utility of morphological and molecular sequence characters in establishing species boundaries in the aseptate gregarine *Lecudina tuzetae* Schrével, 1963. The study is not a good test of the use of morphological or molecular techniques in delineating species because the morphological techniques were inappropriate, sample sizes were too small, and only 1 species was included in the design. The study is limited to 2 populations of a single gregarine species collected from polychete worms near Vancouver, Canada. The morphological methods used fail to recognize or account for known causes of morphotypical variation within a species that are addressed by most standardized protocols in the discipline. For example, morphological sample sizes (in this case, only 5 to 7 individuals for each of 3 morphotypes characterized) were too small to provide an accurate estimate of the population centroid (see Clopton, 2006), and the authors failed to distinguish mature gamonts from immature trophozoites and, thus, introduced developmental variation into the data set (see Filipponi, 1951; Watwood et al., 1997; Clopton, 1999). Moreover, the protocols created obvious osmotic artifacts and variability by failure to correctly fix permanent specimens for mensural data collection (see Clopton, 1999). Rueckert, Villette, and Leander (2011) concluded that both molecular and morphological characters have difficulty delimiting the ''clouds of variation'' associated with morphotype and geography. Unfortunately, their study does not provide a test of species boundaries for either character set: there is only 1 species involved and, thus, the ''clouds of variation'' simply reflect the normal variation within this species.

The study presented herein, and similar published studies (Clopton, 2006; Clopton et al., 2010; Clopton, 2011), clearly demonstrate that morphometric techniques can confidently delimit and describe gregarine species. However, in order to use these techniques to parse meaningful species variation, any morphometric study of gregarine species boundaries must recognize and address 6 principles.

First, delineating species boundaries and describing species is fundamentally a population-level endeavor. The objective is to describe the centroid and normal variation of a population or metapopulation and not to describe an individual. As such, subsequent gregarine identification is also a population-level venture. As is often the case with members of Protista, species-level identification of a single individual is daunting, if not impossible, and is a questionable test of techniques or data used for species recognition and delineation.

Second, sample size must be sufficient to accurately reflect the population centroid and variation of morphometric characters and allow discrimination of underlying categorical shape characters. For each life cycle stage used in a description, the sample size should include at minimum 30–45 individuals so that developmental outliers can be recognized and excluded from the description of normal species variation. Collecting an adequate sample size is rarely problematic in gregarine taxonomy, given the typical intensity and prevalence associated with gregarine infection in an invertebrate population.

Third, careful study of developmental and life cycle stage variation is required in order to correctly identify life cycle stages and select mature, representative specimens for morphometric analysis (see Filipponi, 1951; Watwood et al., 1997; Clopton, 1999). Watwood et al. (1997) demonstrate that most of the gregarines in a population infecting a single host are immature. Mature, and thus morphometrically informative, gamonts make up only a small fraction of the infection in any given host. Immature specimens must be eliminated from the descriptive analysis because they are outliers that shift the centroid and increase the variation of a population, inaccurately representing the normal centroid and variation of the species under study.

Fourth, descriptions must consider, and account for, sexual dimorphism in mature gamonts (Filipponi, 1947, 1951, 1952, 1954, 1955; see Clopton [2009] for a discussion of gamont maturity, gamontic anisomorphy, and the taxonomic issues of precocious association). If sexual dimorphism is apparent, sexes should be analyzed and described separately, but characters from both sexual morphs could be combined to delineate a species boundary (e.g., Fig. 38). In gregarine taxa with isogamonts, no such differentiation is required (e.g., Stylocephalidae and Actinocephalidae).

Fifth, morphometric and categorical shape data must be taken from uniformly prepared specimens with minimal artifacts due to fixation or physiology. These data should be acquired from permanent specimens that have been carefully fixed and stained (Clopton, 1999). Data taken from live specimens should be avoided because they are usually highly variable due to changes in size and shape caused by heat, osmotic differential, and myoneme constriction. At best, variation from these sources can obscure the true population centroid and exaggerate the population variation of a species. At worst, these artifacts lead to the recognition of multiple false morphotypes within a single species.

Finally, any attempt to delimit gregarine species must be comparative and must consider variation in a large character set over multiple life cycle stages. Species that cannot be confidently

distinguished using gamonts or trophozoites may, however, be readily differentiated using oocyst characters alone (e.g., Clopton, 1999). These data must be analyzed in light of comparable data from closely related species. As the study presented herein demonstrates, this often means synoptic collection of new data sets from closely related species because of the limited number of gregarine species for which there is an adequate public specimen base.

ACKNOWLEDGMENTS

This material is based upon work supported in part by the National Science Foundation through grant NSF DEB-1019419. Any opinions, findings, and conclusions or recommendations expressed in this material are those of the author and do not necessarily reflect the views of the National Science Foundation.

LITERATURE CITED

Clopton, R. E. 1995. *Leidyana migrator* n. sp. (Apicomplexa: Leidyanidae) from the Madagascar hissing cockroach, *Gromphadorhina portentosa* (Insecta: Blattodea). Invertebrate Biology **114:** 271–278.

———. 1999. Revision of the genus *Xiphocephalus* and description of *Xiphocephalus ellisi* n. sp. (Apicomplexa: Eugregarinida: Stylocephalidae) from *Eleodes opacus* (Coleoptera: Tenebrionidae) in the western Nebraska Sandhills. Journal of Parasitology **85:** 84–89.

———. 2002. Phylum Apicomplexa Levine, 1970: Order Eugregarinorida Léger, 1900. *In* Illustrated guide to the Protozoa, 2nd ed., J. J. Lee, G. Leedale, D. Patterson, and P. C. Bradbury (eds.). Society of Protozoologists, Lawrence, Kansas, p. 205–288.

———. 2004. Standard nomenclature and metrics of plane shapes for use in gregarine taxonomy. Comparative Parasitology **71:** 130–140.

———. 2006. Two new species of *Xiphocephalus* in *Eleodes tricostata* and *Eleodes fusiformis* (Coleoptera: Tenebrionidae: Eleodini) from the Sandhills of western Nebraska. Journal of Parasitology **92:** 569–577.

———. 2009. Phylogenetic relationships, evolution, and systematic revision of the septate gregarines (Apicomplexa: Eugregarinorida: Septatorina). Comparative Parasitology **76:** 167–190.

———. 2010. *Protomagalhaensia cerastes* n. sp. (Apicomplexa: Eugregarinida: Blabericolidae) parasitizing the pallid cockroach, *Phoetalia pallida* (Dictyoptera: Blaberidae). Comparative Parasitology **77:** 117–124.

———. 2011. Redescription of *Protomagalhaensia granulosae* Peregrine, 1970 (Apicomplexa: Eugregarinida: Blabericolidae) parasitizing the discoid cockroach, *Blaberus discoidalis* (Dictyoptera: Blaberidae). Comparative Parasitology **78:** 63–72.

———, T. J. Cook, and J. J. Cielocha. 2010. *Nubenocephalus nickoli* n. sp. and *Nubenocephalus xunantunichensis* n. sp. (Apicomplexa: Eugregarinida: Actinocephalidae) parasitizing damselflies (Odonata: Zygoptera) in Belize, Central America. Comparative Parasitology **77:** 125–136.

———, and J. J. Hays. 2006. Revision of the genus *Protomagalhaensia* and description of *Protomagalhaensia wolfi* n. comb. (Apicomplexa: Eugregarinida: Hirmocystidae) and *Leidyana haasi* n. comb. (Apicomplexa: Eugregarinida: Leidyanidae) parasitizing the lobster cockroach, *Nauphoeta cinerea* (Dictyoptera: Blaberidae). Comparative Parasitology **73:** 137–156.

Filipponi, A. 1947. *Gregarina dimorpha* n. sp. parassita di *Chlaenius vestitus* Payk. Con osservazioni sulla sua variabilità e sul suo dimorfismo. Rendiconti dell'Accademia Nazionale dei Lincei serie 8 **2:** 856–864.

———. 1951. Su una gregarina (*Gregarina larvarum* n. sp.) rinvenuta in larve di *Blaps gibba* ottenute da allevamento. Rivista di Parassitologia **12:** 85–111.

———. 1952. Accrescimento relativo in due fenotipi di *Protomagalhaensia marottai* Filipponi 1952. Rivista di Parassitologia **13:** 217–234.

———. 1954. Sul dimorfismo sessuale nelle gregarine. Rendiconti dell'Instituto Superiore di Sanità **17:** 908–939.

———. 1955. Dimorfismo sessuale nei trofozoidi del genere *Gigaductus* (Sporozoa, Gregarinida, Gigaductidae). Rendiconti dell'Instituto Superiore di Sanità **18:** 97–114.

Levine, N. D. 1971. Uniform terminology for the protozoan subphylum Apicomplexa. Journal of Protozoology **18:** 352–355.

Peregrine, P. C. 1970. Gregarines found in cockroaches of the genus *Blaberus*. Parasitology **61:** 135–151.

Roth, L. M. 1983. Systematics and phylogeny of cockroaches (Dictyoptera: Blattaria). Oriental Insects **37:** 1–186.

Rueckert, S. and B. S. Leander. 2009. Molecular phylogeny and surface morphology of marine archigregarines (Apicomplexa), *Selenidium* spp., *Filipodium phascolosomae* n. sp., and *Platyproteum* n. g. and comb. from northeastern Pacific peanut worms (Sipuncula). Journal of Eukaryotic Microbiology **56:** 428–439.

———, M. A. H. Villette, and B. S. Leander. 2011. Species boundaries in gregarine apicomplexan parasites: A case study—Comparison of morphometric and molecular variability in *Lecudina* cf. *tuzetae* (Eugregarinorida, Lecudinidae). Journal of Eukaryotic Microbiology **58:** 275–283.

Watwood, S., J. Janovy Jr., E. Peterson, and M. A. Addison. 1997. *Gregarina triboliorum* (Eugregarinida: Gregarinidae) n. sp. from *Tribolium confusum* and resolution of the confused taxonomic history of *Gregarina minuta* Ishii, 1914. Journal of Parasitology **83:** 502–507.